Dalton Transactions

Cite this: DOI: 10.1039/c2dt30448a

www.rsc.org/dalton

PAPER

Fixation of carbon dioxide and related small molecules by a bifunctional frustrated pyrazolylborane Lewis pair†

Eileen Theuergarten, Janin Schlösser, Danny Schlüns, Matthias Freytag, Constantin G. Daniliuc, Peter G. Jones and Matthias Tamm*

Received 24th February 2012, Accepted 17th April 2012
DOI: 10.1039/c2dt30448a

The bifunctional frustrated Lewis pair 1-[bis(pentafluorophenyl)boryl]-3,5-di-*tert*-butyl-1*H*-pyrazole (**1**) was employed for small molecule fixation by reaction with carbon dioxide, paraformaldehyde, *tert*-butyl isocyanate, *tert*-butyl isothiocyanate, methyl isothiocyanate and benzonitrile, affording the adducts **3–8** as zwitterionic, bicyclic boraheterocycles. Treatment of **1** with *tert*-butyl isocyanide gave the isocyanide–borane complex **9**, whereas the zwitterionic alkynylborate **10** was formed by C–H bond activation of phenylacetylene. The molecular structures of all products **3–10** were established by X-ray diffraction analyses. DFT calculations at the M06-2X/6-311++G(d,p) level of theory revealed that CO_2 fixation by **1** and formation of the adduct **3** is strongly exothermic and proceeds with a low energy barrier of approximately 7.3 kcal mol^{-1} *via* an intermediate van der Waals complex.

Introduction

Research on so-called "frustrated Lewis pairs" (FLPs) has witnessed a tremendous increase during the last six years[1] since Stephan's first report on the ability of the intramolecular phosphine–borane FLP system *para*-$(Mes)_2P(C_6F_4)B(C_6F_5)_2$ (Mes = 2,4,6-trimethylphenyl) to cleave dihydrogen under ambient conditions.[2] This unique reactivity results from the prevention of classical adduct formation by use of sterically demanding Lewis acids and bases,[3] and numerous FLP systems have been developed to date by combination of bulky P- or N-donor Lewis bases with polyfluorinated boranes.[4,5] In addition, C-donor Lewis bases such as *N*-heterocyclic carbenes and related species have been employed in combination with $B(C_6F_5)_3$,[6–8] and also alternative Lewis acids such as alanes,[9] silylium ions,[10] or metal-based systems have been used in place of boranes.[11]

For most FLP systems, small molecule activation proceeds in an intermolecular fashion, whereas a significantly smaller number of bifunctional P/B and N/B combinations is known in which the active centres are located close to each other and are therefore able to act simultaneously *and* intramolecularly on other molecules.[12–14] Among these, Erker's ethylene-bridged phosphinoborane $(Mes)_2P\text{-}CH_2CH_2\text{-}B(C_6F_5)_2$ and Rieger's *ortho*-phenylene-bridged 2,2,6,6-tetramethylpiperidinoborane $TMP\text{-}CH_2\text{-}C_6H_4\text{-}B(C_6F_5)_2$ represent the most prominent examples,[13,14] and it was shown that both FLP systems can activate H_2 and even act as metal-free catalysts for the hydrogenation of imines and other substrates.[15] Similarly, we were able to show that the pyrazolylborane **1**, in agreement with theoretical predictions for related molecules,[16] is able to promote heterolytic dihydrogen cleavage under ambient conditions; the resulting zwitterionic pyrazolium–hydroborate **2** shows potential for catalytic imine reduction (Scheme 1).[17] In continuation of this work, we decided to investigate the fixation of other small molecules by FLP **1**, since in particular Erker's and related intramolecular P/B systems exhibit a rich chemistry towards substrates such as olefins,[18] alkynes,[18,19] carbon dioxide,[20,21] isocyanates,[20,22] azides,[22] and singlet dioxygen.[23] In addition, CO_2 fixation and activation of other small molecules was also reported for several geminal P/B- and P/Al-based systems in which the spatial arrangement of the donor and acceptor sites is similar to that in **1**.[24,25]

It should be emphasized that CO_2 fixation by intramolecular boron–nitrogen FLP systems has not been previously reported, except for the reaction of CO_2 with four-membered boron amidinates by insertion into one of the B–N bonds.[26] Therefore, studying the reactivity of **1** towards CO_2 and related substrates is of

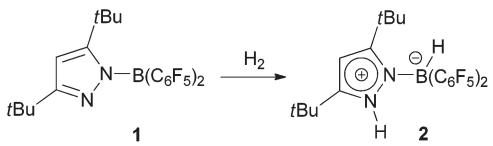

Scheme 1 Intramolecular heterolytic dihydrogen cleavage promoted by FLP **1**.

Institut für Anorganische und Analytische Chemie, Technische Universität Carolo-Wilhelmina, Hagenring 30, D-38106 Braunschweig, Germany. E-mail: m.tamm@tu-bs.de; Fax: +49 531-391-5309; Tel: +49 531-391-5387

†Electronic supplementary information (ESI) available: Details of the electronic structure calculations and presentations of all calculated structures together with Cartesian coordinates of their atomic positions. CCDC 869097–869104. For ESI and crystallographic data in CIF or other electronic format see DOI: 10.1039/c2dt30448a

substantial interest, particularly in view of its potential for the development of non-metal-mediated procedures for the selective hydrogenation or hydrosilylation of CO_2, as was recently demonstrated for the intermolecular B/N combination 2,2,6,6-tetramethylpiperidine/$B(C_6F_5)_3$.[27,28] Accordingly, we report herein the reactions of **1** with the small molecules carbon dioxide and formaldehyde and also with organic isocyanates, isothiocyanates, nitriles, isonitriles and alkynes.

Results and discussion

Carbon dioxide fixation

A pale yellow toluene solution of the pyrazolylborane **1** was exposed to carbon dioxide gas at room temperature, immediately affording a colourless solution. After stirring for 10 minutes, evaporation and rinsing with pentane gave the zwitterionic carbon dioxide adduct **3** as a white solid in 90% yield (Scheme 2). Whereas **1** shows only one set of resonances for the *t*Bu groups in the ^{1}H NMR spectra because of rapid exchange of the $B(C_6F_5)_2$ group between the two nitrogen atoms,[17] **3** gives rise to two separate signals at 1.06 and 1.45 ppm. The ^{11}B NMR resonance is shifted from +43.1 in **1** to +2.3 ppm in **3**, which indicates a transition from a trigonal planar towards a tetrahedral coordination sphere of the boron atom. The ^{13}C NMR signal of the quaternary carbon atom of the fixed CO_2 molecule appears at 144.6 ppm, which is in agreement with the resonance reported for a six-membered heterocycle formed by insertion of CO_2 into the B–N bond of a boron amidinate.[26] The observation of one ^{19}F resonance each for the *ortho*-, *para*-, and *meta*-fluorine atoms at −135.5, −154.9 and −163.5 ppm, respectively, reveals free rotation around the B–C bonds at room temperature on the NMR time scale. In the IR spectrum, the CO stretching frequency is found in the expected range at 1803 cm^{-1}.

The molecular structure of **3** was established by X-ray diffraction analysis (Fig. 1), confirming the formation of the bicyclic product **3** with two almost coplanar five-membered heterocycles. The boracycle formed by CO_2 addition displays a comparatively high degree of asymmetry with markedly different intraring bond distances and angles, displaying for instance a small N1–B–O1 angle of 98.05(10)° next to a rather obtuse B–O1–C12 angle of 114.90(11)°. The B–O1 bond length of 1.5063(18) Å is similar to that reported for the six-membered CO_2-boron amidinate adduct [1.493(5) Å] (*vide supra*),[26] whereas significantly longer B–O bonds were found for CO_2 adducts of the intramoluclar P/B systems (*t*Bu)$_2$P-CH_2-BPh_2 [1.5645(15) Å][20] and $(Mes)_2$P-CH_2CH_2-$B(C_6F_5)_2$ [1.550(4) Å].[21] In agreement with the previously described CO_2 adducts, the C12–O2 and C12–O1 bond lengths of 1.1936(16) and 1.3067(16) Å exhibit the expected predominantly double- and single-bond character, respectively.

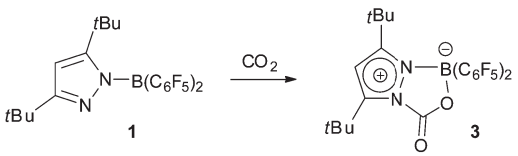

Scheme 2 Carbon dioxide fixation by FLP **1**.

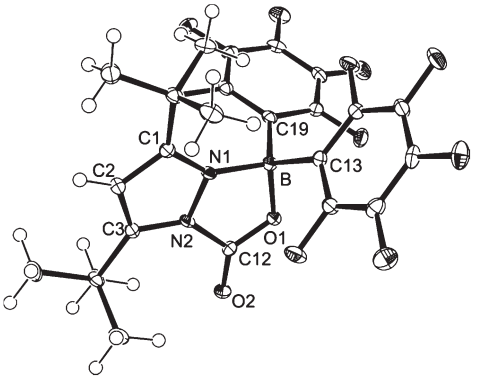

Fig. 1 ORTEP diagram of **3** with thermal displacement parameters drawn at 50% probability. Selected bond lengths (Å) and angles (°): B–O1 1.5063(18), B–N1 1.5946(18), B–C13 1.624(2), B–C19 1.631(2), N1–C1 1.3404(18), N1–N2 1.3735(15), N2–C3 1.3667(17), N2–C12 1.4428(17), O1–C12 1.3067(16), O2–C12 1.1936(16); O1–C12–O2 128.19(13), C12–O1–B 114.90(11), O1–B–N1 98.05(10), O1–B–C13 109.71(11), N1–B–C13 110.21(11), O1–B–C19 106.28(11), N1–B–C19 113.57(11), C13–B–C19 117.15(11).

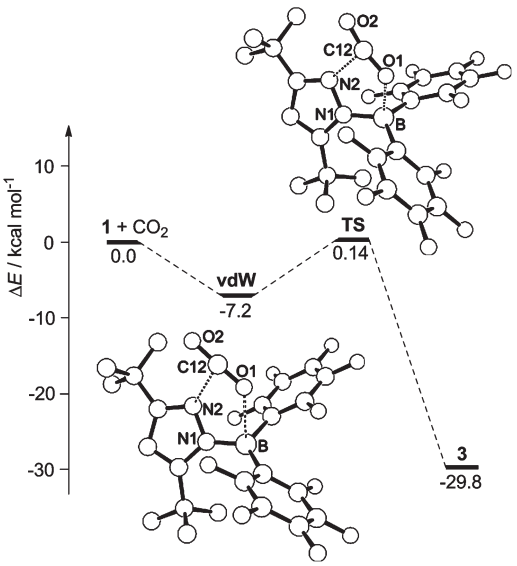

Fig. 2 Relative energies (kcal mol^{-1}) for stationary points on the **1** + CO_2 hypersurface. Values correspond to ΔE = zero-point uncorrected M06-2X/6-311++G(d,p) electronic energies. PLUTO drawings of the van der Waals complex (vdW) and the transition state (TS). Selected bond lengths (Å) and angles (°): vdW: B–O1 2.814, N2–C12 2.909, C12–O1 1.158, C12–O2 1.154, O1–C12–O2 177.4; TS: B–O1 1.954, N2–C12 2.266, C12–O1 1.192, C12–O2 1.149, O1–C12–O2 164.2.

The CO_2 adduct **3** was thermally stable under vacuum at elevated temperature and showed no sign of CO_2 release. This irreversible carbon dioxide binding was further investigated by DFT calculations; the optimized structures of **1** and **3** agree well with data derived from X-ray diffraction analysis (*vide supra*; see ESI† for a presentation of all calculated structures).[17] The formation of **3** was calculated to be strongly exothermic (ΔE = −29.8 kcal mol^{-1}), which is in agreement with the experimentally observed irreversible CO_2 fixation (Fig. 2). Similarly, the

structurally related adduct isolated from $(t\text{Bu})_2\text{P-CH}_2\text{-BPh}_2$ showed no release of CO_2, and calculations at a similar level of theory also revealed a high stability of this adduct (ΔE = −20.3 kcal mol^{-1}).[20] In contrast, CO_2 fixation with $(\text{Mes})_2\text{P-CH}_2\text{CH}_2\text{-B}(\text{C}_6\text{F}_5)_2$ was calculated to be almost thermoneutral (ΔE = −2.9 kcal mol^{-1}), in accord with the experimentally observed reversibility.[21]

By analogy to the reaction pathways theoretically derived for these P/B Lewis pairs and also for a related geminal P/Al-based FLP,[20,21,25b] our calculations revealed the occurrence of an intermediate van der Waals complex (vdW, ΔE = −7.2 kcal mol^{-1}) with an almost linear CO_2 molecule (177.4°). The B–O1 and N2–C12 distances of 2.814 and 2.909 Å in this complex become progressively shorter upon conversion into **3** (B–O1 = 1.503 Å, N2–C12 = 1.455 Å, O1–C12–O2 = 129.3°) *via* a transition state (TS, ΔE = +0.14 kcal mol^{-1}) that lies only 7.3 kcal mol^{-1} above the van der Waals complex (vdW). The resulting B–O1 (1.954 Å) and N2–C12 (2.266 Å) bonds are long and—together with short C–O bonds of 1.182 (C12–O1) and 1.149 Å (C12–O2) and a large O–C–O angle of 164.2°—correspond to an "early" transition state. The reverse reaction and release of CO_2 from **3** requires an activation energy of approximately 30 kcal mol^{-1}, which is consistent with the experimentally observed irreversibility of the CO_2 fixation (*vide supra*).

Fixation of formaldehyde

Since formaldehyde represents a possible intermediate during non-metal mediated homogeneous hydrogenation of CO_2 to CH_3OH,[27] we attempted the fixation of this small molecule by **1**. Hence, a toluene solution of **1** was treated with an excess of paraformaldehyde ($C_3H_6O_3$). The pale yellow solution became colourless after stirring the mixture for one hour at room temperature, and the bicyclic product **4** was isolated in almost quantitative yield as a white solid after evaporation and extraction with pentane (Scheme 3). The ^{11}B NMR resonance at 2.5 ppm appears in the same high-field range as observed for **3** (*vide supra*). The signals for the CH_2 moiety are found at 5.56 and 78.6 ppm in the ^{1}H and ^{13}C NMR spectra, respectively. Similarly to **3**, two separate ^{1}H NMR resonances are observed for the *t*Bu groups at 0.97 and 1.29 ppm, and the ^{19}F NMR spectrum is also almost identical.

Crystals of **4**·1/2(toluene) suitable for X-ray diffraction analysis were obtained from a mixture of toluene–hexane at −30 °C, and the molecular structure of **4** is shown in Fig. 3. The five-membered boracycle adopts an envelope conformation, whereby the oxygen atom lies 0.46 Å out of the B–N1–N2–C12 plane; the resulting B–O bond of 1.4769(14) Å in **4** is slightly shorter than in **3** [1.5063(18) Å]. The bond angles at the boron atom range from 98.57(8)° (N1–B–O) to 112.72(9)° (C13–B–C19), indicating a distorted tetrahedral coordination sphere.

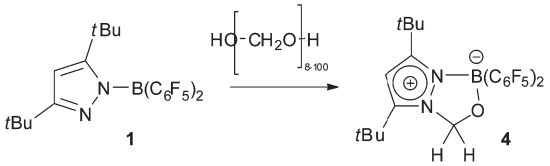

Scheme 3 Fixation of formaldehyde by FLP **1**.

Fixation of isocyanates and isothiocyanates

To investigate the fixation of other small molecules that are (valence) isoelectronic with carbon dioxide, **1** was also reacted with organic isocyanates and isothiocyanates, which can potentially lead to different regioisomers by N or O/S coordination to the Lewis acidic boron site. Treatment of a toluene solution of **1** with *tert*-butyl isocyanate (*t*BuNCO) afforded the adduct **5** as a white solid in 76% yield (Scheme 4). The ^{1}H NMR spectra indicated the formation of a new product by showing three signals for the *t*Bu groups at 0.83, 1.39 and 1.44 ppm; two-dimensional NMR spectroscopy (HMBC experiment) allowed the assignment of the resonance at 1.39 ppm to the *t*Bu group of the inserted isocyanate. Similarly to the formation of **3** and **4**, the ^{11}B NMR peak is shifted up-field to 2.5 ppm upon isocyanate coordination. Finally, the ^{13}C NMR resonance of the quarternary carbon atom of the NCO moiety is found at 139.8 ppm.

X-Ray diffraction analysis allowed the determination of the molecular structure of **5** (Fig. 4), revealing the incorporation of the isocyanate CO group into the five-membered ring.

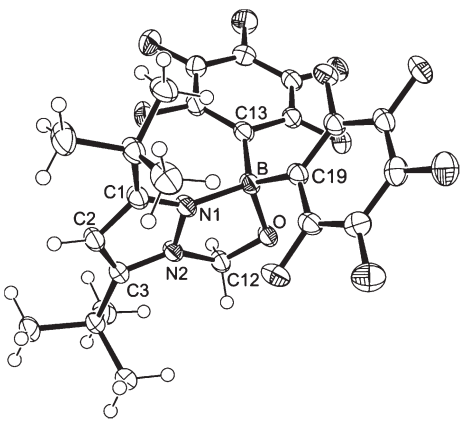

Fig. 3 ORTEP diagram of **4** with thermal displacement parameters drawn at 50% probability. Selected bond lengths (Å) and angles (°): B–O 1.4769(14), B–N1 1.6087(14), B–C19 1.6293(17), B–C13 1.6429 (17), N1–C1 1.3488(14), N1–N2 1.3617(13), N2–C3 1.3460(14), N2–C12 1.4793(13), O–C12 1.3865(13); O–B–N1 98.57(8), O–B–C19 106.67(9), N1–B–C19 112.72(9), O–B–C13 108.48(9), N1–B–C13 111.40(9), C19–B–C13 117.13(9), C12–O–B 109.65(8).

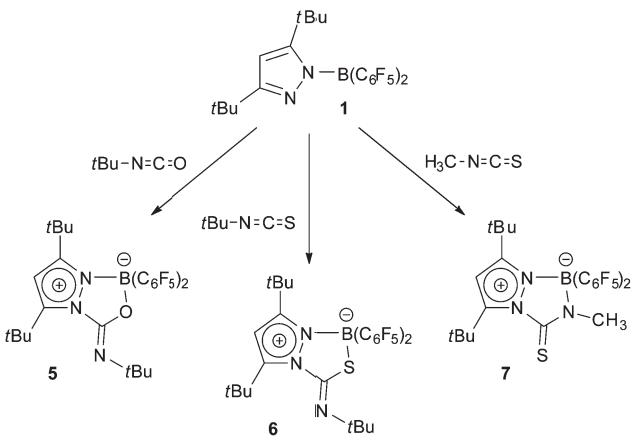

Scheme 4 Fixation of isocyanates and isothiocyanates by FLP **1**.

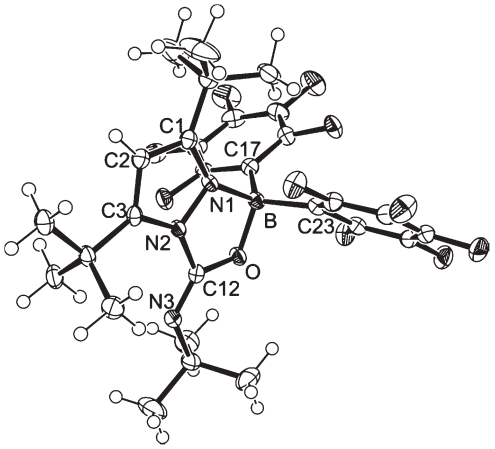

Fig. 4 ORTEP diagram of **5** with thermal displacement parameters drawn at 50% probability. Selected bond lengths (Å) and angles (°): B–O 1.4937(19), B–N1 1.5924(19), B–C23 1.628(2), B–C17 1.631(2), N1–C1 1.3386(18), N1–N2 1.3742(16), N2–C3 1.3637(18), N2–C12 1.4478(18), N3–C12 1.2499(19), O–C12 1.3254(17); O–B–N1 98.26 (11), O–B–C23 105.31(12), N1–B–C23 113.88(12), O–B–C17 108.80 (12), C1–N1–N2 108.03(11), C1–N1–B 144.02(12), N2–N1–B 107.95 (11), N1–N2–C12 110.53(11), C12–O–B 115.10(11), C12–N3–C13 120.75(13).

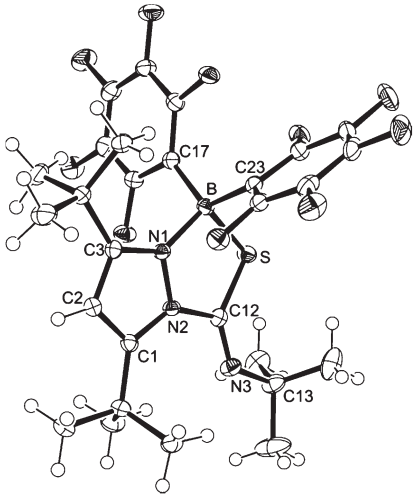

Fig. 5 ORTEP diagram of **6** with thermal displacement parameters drawn at 50% probability. Selected bond lengths (Å) and angles (°): S–C12 1.7533(11), S–B 1.9479(12), B–N1 1.5744(14), B–C23 1.6280 (16), B–C17 1.6287(16), N1–C3 1.3445(14), N1–N2 1.3807(12), N2–C1 1.3737(14), N2–C12 1.4560(14), N3–C12 1.2518(15), N3–C13 1.4879(15); C12–S–B 94.84(5), N1–B–C23 112.72(9), N1–B–C17 109.33(9), C23–B–C17 119.06(9), N1–B–S 100.54(7), C23–B–S 104.79(7), C17–B–S 108.57(7), C3–N1–N2 108.10(8), C12–N3–C13 125.19(10).

Accordingly, the overall structural parameters of the bicyclic system are very similar to those established for the CO_2 adduct **3**, with the newly formed B–O and N2–C12 bonds of 1.4937 (19) and 1.4478(18) Å being almost identical to those in **3**. The exocyclic imine moiety exhibits a very short C12–N3 bond of 1.2499(19) Å in agreement with the presence of a C–N double bond. The C–N–C angle at N3 is 120.75(13)°, and the *t*Bu group at N3 adopts an *E*-configuration with respect to the pyrazole ring.[20,22]

The reaction of **1** with isothiocyanates was also studied, since these molecules exhibit two distinctly different binding sites according to Pearson's acid–base concept and could therefore bind to the hard boron Lewis acid either through the soft sulfur atom or through the hard, but sterically more encumbered nitrogen atom.[30] Addition of *tert*-butyl isothiocyanate to a toluene solution of **1** afforded a white solid in almost quantitative yield after stirring for 15 minutes and work-up by evaporation and washing with pentane (Scheme 4). Again, NMR spectroscopy indicates the formation of a single addition product, with the ^{1}H NMR resonances of the *t*Bu groups of the pyrazole ring at 0.82 and 1.39 ppm and that of the additional *t*Bu group at 1.33 ppm. At −3.3 ppm, the ^{11}B NMR resonance appears at higher field compared to the corresponding isocyanate adduct **5**. In the ^{13}C NMR spectrum, the resonance of the quaternary carbon atom of the NCS moiety is found at 146.2 ppm.

Single crystals of **6** could be obtained from a toluene–hexane solution at −30 °C, and X-ray diffraction analysis confirmed the formation of the bicyclic addition product with incorporation of the CS fragment into the five-membered boracycle (Fig. 5). Compared to the isocyanate congener **5**, introduction of the sulfur atom leads to a stronger deviation from planarity and to a noticeable distortion towards an envelope conformation, whereby the sulfur atom lies 0.24 Å out of the B–N1–N2–C12 plane. Clearly, the B–S and C12–S bond lengths of 1.9479(12) and 1.7533(11) Å are longer than the corresponding B–O and C–O bonds in **5**, affording a B–S–C12 angle of 94.84(5)° that is smaller than the B–O–C12 angle of 115.10(11)° in **5**.

The molecular structure of **6** revealed an apparent mismatch of the soft Lewis basic sulfur atom with the hard Lewis acidic boron atom, which might be a result of the steric congestion at the nitrogen atom in *t*BuNCS. Therefore, the reaction of **1** with methyl isothiocyanate was additionally investigated, which might favour B–N bond formation. Indeed, the ^{13}C NMR resonance of the quarternary NCS carbon atom is observed at 171.3 ppm at significantly lower field than the corresponding resonance in **6**, which indicates the presence of a thiocarbonyl moiety and formation of the bicyclic boratriazole **7** (Scheme 4). The ^{11}B NMR shift is detected at −1.8 ppm, and the ^{1}H NMR spectrum exhibits characteristic singlets at 0.71, 1.63 and 3.09 ppm for the *t*Bu and CH_3 groups, respectively.

The formation of **7** was confirmed by X-ray diffraction analysis (Fig. 6); the N2–C12 and B–N3 bond lengths are 1.4410(15) and 1.5525(16) Å, with the latter being slightly shorter than the B–N bond reported for isocyanate adduct of a geminal P/B frustrated Lewis pair [1.580(5) Å].[24b] The exocyclic C–S bond length of 1.6507(12) Å falls in the range (mean distance = 1.671 Å) established for compounds of the type $(X)_2$–C═S (X = C, N, O, S).[31]

Fixation of nitriles and isonitriles

The reactivity of the FLP **1** towards organic nitriles and isonitriles was also studied in order to investigate potential BN addition across the R–C≡N or R–N≡C moieties. Hence, addition of benzonitrile (PhCN) to a toluene solution of **1**

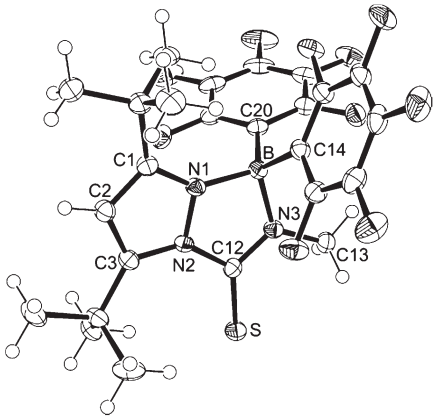

Fig. 6 ORTEP diagram of **7** with thermal displacement parameters drawn at 50% probability. Selected bond lengths (Å) and angles (°): S–C12 1.6507(12), B–N3 1.5525(16), B–N1 1.5851(16), B–C14 1.6369 (17), B–C20 1.6400(17), N1–C1 1.3445(15), N1–N2 1.3868(13), N2–C3 1.3735(15), N2–C12 1.4410(15), N3–C12 1.3289(15), N3–C13 1.4513(15); N3–B–N1 95.85(8), N3–B–C14 112.66(10), N1–B–C14 109.13(9), N3–B–C20 107.03(9), N1–B–C20 114.41(10), C14–B–C20 116.00(10), C13–N3–B 124.81(9), C12–N3–B 115.96(10).

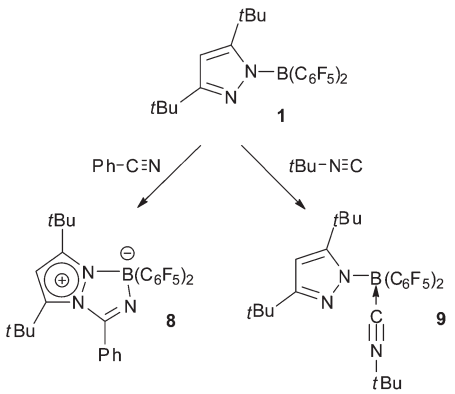

Scheme 5 Nitrile and isonitrile fixation by FLP **1**.

afforded a white solid in 85% yield. The signals in the ^{1}H and ^{13}C NMR spectra are broadened, indicating a dynamic process in solution. A ^{13}C NMR resonance at 133.4 ppm can tentatively be assigned to the quarternary nitrile carbon atom, which is at lower field compared to the chemical shift (121.1 ppm) reported for the pivalonitrile adduct $(Mes)_2P\text{-}CH_2CH_2\text{-}B(C_6F_5)_2(NC\textit{t}Bu)$, which shows no interaction between the Lewis basic phosphorus atom and the boron-bound nitrile molecule in the solid state.[22] Accordingly, 1,2-addition of **1** across the CN bond and formation of the boratriazole **8** could be expected (Scheme 5), which was unambiguously confirmed by X-ray diffraction analysis.

The molecular structure of **8** is shown in Fig. 7; the B–N3 bond in **8** [1.529(2) Å] is slightly longer than the corresponding B–N bond in the six-membered boron amidinate–acetonitrile adduct [1.5147(11) Å],[26] but shorter than the B–N3 bond in **7** [1.5525(16) Å], which contains a nitrogen-bound methyl group (*vide supra*). The pivalonitrile adduct $(Mes)_2P\text{-}CH_2CH_2\text{-}B(C_6F_5)_2(NC\textit{t}Bu)$, in which the nitrile interacts only with the Lewis acidic boron site, exhibits a significantly longer B–N

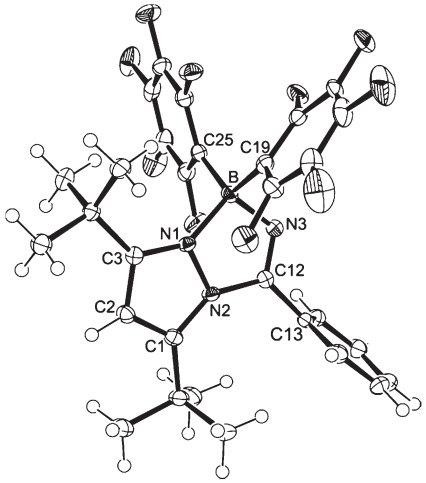

Fig. 7 ORTEP diagram of **8** with thermal displacement parameters drawn at 50% probability. Selected bond lengths (Å) and angles (°): N1–C3 1.343(2), N1–N2 1.3842(17), N1–B 1.606(2), N2–C1 1.375(2), N2–C12 1.477(2), N3–C12 1.255(2), N3–B 1.529(2), C1–C2 1.376(2), C12–C13 1.487(2), B–C19 1.624(4), B–C25 1.634(2); C3–N1–N2 108.32(12), C3–N1–B 143.79(13), N2–N1–B 107.73(11), C12–N3–B 111.49(13), N3–C12–N2 113.89(14), N3–C12–C13 122.08(14), N3–B–N1 99.70(12), N3–B–C19 102.5(2), N1–B–C19 115.8(2), N3–B–C25 111.50(13), N1–B–C25 109.32(13), C19–B–C25 116.4(2).

bond of 1.588(5) Å and a C–N bond length of 1.136(4) Å consistent with a triple bond,[22] whereas the C12–N3 distance in **8** [1.255(2) Å] corresponds to a double bond.

In contrast to the formation of a five-membered ring by 1,2-addition of **1** across the C–N bond in benzonitrile (*vide supra*), the interaction of **1** with isonitriles could be expected to afford a strained four-membered ring by 1,1-addition to the terminal carbon atom.[32] However, addition of *tert*-butyl isocyanide to a toluene solution of **1** gave a white solid in almost quantitative yield, which showed a strong absorption at 2302 cm^{-1} in the IR spectrum, indicating the presence of a boron-bound isocyanide ligand. Similarly, a CN stretching frequency of 2287 cm^{-1} was reported for the P/B system $(C_6H_2Me_3)_2P\text{-}CH_2CH_2\text{-}B(C_6F_5)_2(CN\textit{t}Bu)$, in which the isocyanide ligand interacts solely with the boron atom.[22] Formation of the adduct **9** is also confirmed by NMR spectroscopy (Scheme 5), *e.g.* by observation of three singlets in the ^{1}H NMR spectrum at 0.93, 0.98 and 1.42 ppm for the three different *t*Bu groups. The ^{11}B NMR resonance is found at −9.0 ppm, whereas no ^{13}C NMR signal could be observed for the boron-bound carbon atom.

Suitable crystals of **9**·1/2(toluene) for X-ray diffraction analysis were grown from a toluene solution at −30 °C, and the molecular structure of **9** reveals a *t*BuNC ligand that is coordinated in a linear fashion [B–C12–N3 = 173.1(2)°, C12–N3–C13 = 177.5(2)°] (Fig. 8). The B–C12 and C12–N3 bond lengths of 1.641(3) and 1.141(3) Å fall in the range established for related isocyanide–borane adducts.[22,32–34]

Fixation of phenylacetylene

The reactivity of FLPs with terminal alkynes was shown to proceed either proceed *via* terminal C–H activation or *via*

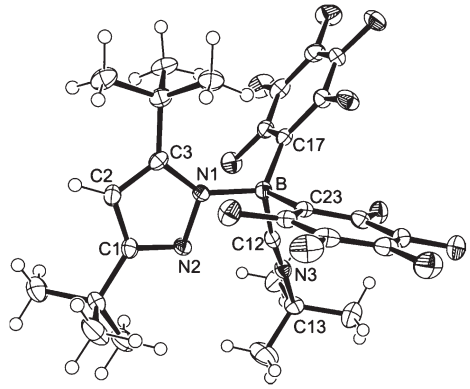

Fig. 8 ORTEP diagram of **9** with thermal displacement parameters drawn at 50% probability. Selected bond lengths (Å) and angles (°): B–N1 1.534(3), B–C17 1.637(3), B–C23 1.641(3), B–C12 1.641(3), N1–C1 1.382(3), N1–N2 1.386(2), N2–C3 1.326(3), N3–C12 1.141(3), N3–C13 1.468(3); N1–B–C17 115.92(18), N1–B–C23 114.89(19), C17–B–C23 114.71(18), N1–B–C12 102.41(18), C17–B–C12 103.48 (18), C23–B–C12 102.77(17), C1–N1–N2 109.48(17), C1–N1–B 138.86(18), C12–N3–C13 177.5(2).

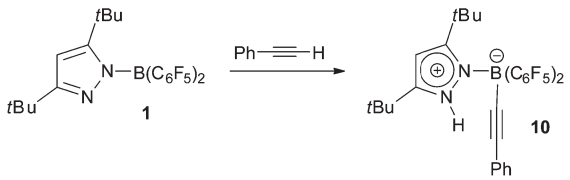

Scheme 6 C–H activation and phenylacetylene fixation by FLP **1**.

1,2-addition with formation of zwitterionic alkenes.[12c,24b,34] Thus, the reactivity of **1** towards phenylacetylene was studied by stirring a solution of both compounds in toluene for two hours at ambient temperature. The ^{1}H NMR spectrum of the white solid that was obtained in 84% yield showed a broad low-field resonance at 12.20 ppm, indicating the formation of the protonated pyrazolium species **10** by heterolytic C–H bond activation (Scheme 6). Similar reactivity was observed for intramolecular P/B and N/B FLP systems,[12c,18] which exhibit high-field ^{11}B NMR resonances in a similar range as found for **10** (−8.9 ppm), suggesting the presence of an alkynyl borate moiety. This structural assignment was confirmed by X-ray diffraction analysis of **10**·toluene (Fig. 9), and the linearly bound PhCC moiety (B–C12–C13 = 176.25(11)°, C12–C13–C14 = 178.75(11)° displays a B–C12 bond length of 1.5921(15) Å, which is similar to that established for related phenylalkynylborate systems.[8,12c,35]

Conclusions

The bifunctional frustrated pyrazolylborane Lewis pair **1** was successfully employed for the fixation of carbon dioxide and related small molecules. In **1**, the Lewis basic nitrogen atom and the Lewis acidic boron atom are ideally oriented (or preorganized)[20] for the interaction with an incoming ambiphilic molecule such as CO_2. A very low barrier was calculated for the formation of the CO_2 adduct **3**, and it is a reasonable assumption that the fixation of other substrates, such as formaldehyde, isocyanates, isothiocyanates, nitriles, isonitriles and alkynes, also

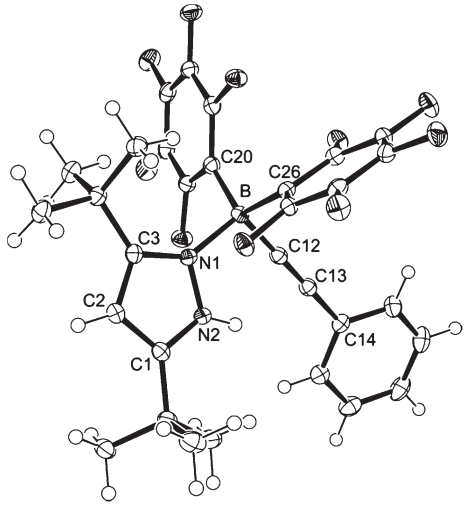

Fig. 9 ORTEP diagram of **10** with thermal displacement parameters drawn at 50% probability. Selected bond lengths (Å) and angles (°): C12–C13 1.2065(16), C13–C14 1.4376(15), B–C12 1.5921(15), B–N1 1.6229(14), B–C20 1.6400(15), B–C26 1.6459(15), N1–N2 1.3627(12), N1–C3 1.3644(13), N2–C1 1.3338(13); C12–B–N1 105.46(8), C12–B–C20 107.90(8), N1–B–C20 110.10(8), C12–B–C26 104.26(8), N1–B–C26 111.85(8), C20–B–C26 116.44(8), C13–C12–B 176.25(11), C12–C13–C14 178.75(11).

requires only small activation energies, as experimentally evidenced by the ease of formation of the adducts **4–10**. CO_2 fixation also proved to proceed in a strongly exothermic manner, affording a highly stable adduct **3**, which showed no release of CO_2. Therefore, fine-tuning and balancing of the Lewis acidity and basicity of pyrazolylboranes related to **1** might lead to less strong and consequently reversible CO_2 binding. In combination with dihydrogen activation,[17] the design of metal-free catalysts for CO_2 hydrogenation can be envisaged.[27–29]

Experimental section

General procedures

All operations with air and moisture-sensitive compounds were performed in a glove box under a dry argon atmosphere (MBraun 200B) or on a high vacuum line using Schlenk techniques. Carbon dioxide gas was purchased from Westfalen AG and passed through a P_4O_{10} column prior to use. All solvents were purified by a solvent purification system from MBraun and stored over molecular sieves (4 Å). The ^{1}H, ^{13}C, ^{11}B, and ^{19}F NMR spectra were recorded on Bruker DPX 200, Bruker AV 300 and Bruker DRX 400 spectrometers. Tetramethylsilane (TMS) was used as internal standard for ^{1}H and ^{13}C. Trichlorofluoromethane ($CFCl_3$) and boron trifluoride diethyletherate (BF_3·OEt_2) were used as external reference for the ^{19}F and ^{11}B NMR spectra, respectively. Chemical shifts are reported in ppm (parts per million). Coupling constants (*J*) are reported in Hertz (Hz), and splitting patterns are indicated as s (singlet), d (doublet), t (triplet), q (quartet), m (multiplet), sept (septet) and br (broad). Elemental analysis was carried out with a Vario Micro Cube System. A Bruker Vertex 70 spectrometer was used for recording the IR spectra. Unless otherwise indicated, all starting materials were obtained from Aldrich and were used without

further purification. The pyrazolylborane **1** was prepared according to a published procedure.[17] All used glassware was silylated prior to use, and toluene was dried over sodium–potassium alloy.

Synthesis and characterisation of the CO_2 adduct 3

A toluene solution (15 mL) of **1** (182 mg, 0.35 mmol) was purged with CO_2 for 10 minutes at room temperature. The pale yellow solution became colourless within one minute. After stirring the mixture for one hour under CO_2 atmosphere, the solvent was removed under vacuum. The residue was washed with pentane (5 mL) and dried under vacuum to yield **3** as a white powder (179 mg, 90%). Crystals suitable for X-ray diffraction analysis were obtained from a mixture of CH_2Cl_2 and *n*-hexane at −30 °C. ^{1}H NMR (400 MHz, CD_2Cl_2): δ/ppm 1.06 (s, 9H, CH_3), 1.45 (s, 9H, CH_3), 6.41 (s, 1H, C*H*); ^{11}B NMR (128 MHz, CD_2Cl_2): δ/ppm 2.3 (s); ^{13}C NMR (100 MHz, CD_2Cl_2): δ/ppm 28.6 (CH_3, Me), 29.6 (CH_3, Me), 33.5 (C_q, *C*Me$_3$), 33.8 (C_q, *C*Me$_3$), 111.1 (CH, C═*C*HC), 137.8 (C_q, d, $^1J_{CF}$ = 250 Hz *meta*-C_6F_5), 141.7 (C_q, d, $^1J_{CF}$ = 256 Hz *para*-C_6F_5), 144.6 (C_q, N*C*OO), 148.8 (C_q, d, $^1J_{CF}$ = 252 Hz, *ortho*-C_6F_5), 157.9 (C_q, N═*C*CCH), 162.5 (C_q, N═*C*CCH); ^{19}F NMR (376 MHz, CD_2Cl_2): δ/ppm −135.5 (m, $^3J_{FF}$ = 18.7 Hz, 4F, *o*-C_6F_5), −154.9 (m, $^3J_{FF}$ = 20.4 Hz, 2F, *p*-C_6F_5), −163.5 (m, 4F, *m*-C_6F_5); elemental analysis (%) calculated for $C_{24}H_{19}BF_{10}N_2O_2$: C 50.7, H 3.3, N 4.9, found: C 50.5, H 3.6, N 4.8. IR (ATR): $1/\lambda$/cm^{-1} 2979 (w), 1803 (s), 1647 (w), 1519 (s), 1462 (s), 1106 (s), 958 (s).

Synthesis and characterisation of the CH_2O adduct 4

A toluene solution (5 mL) of **1** (250 mg, 0.48 mmol) was treated with paraformaldehyde (14 mg, 0.48 mmol). The pale yellow solution became colourless after stirring the mixture at room temperature for one hour. The reaction mixture was stirred overnight, whereupon a light precipitate formed. The solvent was removed under vacuum, and the residue was washed with pentane (2 mL). After drying under vacuum, **4** was isolated as a white powder in almost quantitative yield (260 mg, 97%). Crystals suitable for X-ray diffraction analysis were obtained from a mixture of toluene and *n*-hexane at −30 °C. ^{1}H NMR (400 MHz, CD_2Cl_2): δ/ppm 0.97 (s, 9H, CH_3), 1.29 (s, 9H, CH_3), 5.56 (s, 2H, CH_2), 6.19 (s, 1H, C*H*); ^{11}B NMR (128 MHz, CD_2Cl_2): δ/ppm 2.5 (s); ^{13}C NMR (100 MHz, CD_2Cl_2): δ/ppm 29.1 (CH_3, Me), 29.8 (CH_3, Me), 31.9 (C_q, *C*Me$_3$), 32.9 (C_q, *C*Me$_3$), 78.6 (CH_2, N*C*H$_2$O), 107.3 (CH, C═*C*HC), 116.9 (C_q, B*C*$_{ipso}$), 137.5 (C_q, d, $^1J_{CF}$ = 250 Hz *meta*-C_6F_5), 140.9 (C_q, d, $^1J_{CF}$ = 252 Hz *para*-C_6F_5), 149.0 (C_q, d, $^1J_{CF}$ = 243 Hz, *ortho*-C_6F_5), 151.2 (C_q, N═*C*CCH), 156.8 (C_q, N═*C*CCH); ^{19}F NMR (376 MHz, CD_2Cl_2): δ/ppm −135.3 (m, 4F, *o*-C_6F_5), −157.6 (m, $^3J_{FF}$ = 20.5 Hz, 2F, *p*-C_6F_5), −164.7 (m, 4F, *m*-C_6F_5); elemental analysis (%) calculated for $C_{24}H_{21}BF_{10}N_2O$: C 52.0, H 3.8, N 5.1, found: C 52.3, H 4.1, N 4.9.

Synthesis and characterisation of the *t*BuNCO adduct 5

A toluene solution (5 mL) of **1** (279 mg, 0.53 mmol) was treated with *tert*-butyl isocyanate (53 mg, 0.53 mmol). The mixture was stirred for 3 days at room temperature. The solvent was removed under vacuum, and the residue was washed with pentane (3 mL). After drying under vacuum, **5** was isolated as a white powder (254 mg, 76%). Crystals suitable for X-ray diffraction analysis were obtained from a mixture of toluene and *n*-hexane at −30 °C. ^{1}H NMR (400 MHz, C_6D_6): δ/ppm 0.83 (s, 9H, CH_3), 1.38 (s, 9H, CH_3), 1.44 (s, 9H, CH_3), 6.07 (s, 1H, C*H*); ^{11}B NMR (128 MHz, C_6D_6): δ/ppm 2.5 (s); ^{13}C NMR (100 MHz, C_6D_6): δ/ppm 28.3 (CH_3, Me), 29.3 (CH_3, Me (*t*BuNCO)), 29.8 (CH_3, Me), 32.8 (C_q, *C*Me$_3$), 33.5 (C_q, *C*Me$_3$), 54.1 (C_q, *C*Me$_3$ (*t*BuNCO)), 109.4 (CH, C═*C*HC), 116.2 (C_q, B*C*$_{ipso}$), 137.6 (C_q, d, $^1J_{CF}$ = 251 Hz *meta*-C_6F_5), 139.8 (C_q, N*C*O), 141.2 (C_q, d, $^1J_{CF}$ = 248 Hz *para*-C_6F_5), 148.9 (C_q, d, $^1J_{CF}$ = 241 Hz, *ortho*-C_6F_5), 155.5 (C_q, N═*C*CCH), 158.3 (C_q, N═*C*CCH); ^{19}F NMR (376 MHz, C_6D_6): δ/ppm −136.0 (m, 4F, *o*-C_6F_5), −154.8 (m, $^3J_{FF}$ = 21.0 Hz, 2F, *p*-C_6F_5), −163.4 (m, 4F, *m*-C_6F_5); elemental analysis (%) calculated for $C_{28}H_{28}BF_{10}N_3O$: C 54.0, H 4.5, N 6.7, found: C 54.1, H 4.6, N 6.6.

Synthesis and characterisation of the *t*BuNCS adduct 6

A toluene solution (5 mL) of **1** (250 mg, 0.48 mmol) was treated with *tert*-butyl isothiocyanate (53 mg, 0.55 mmol). The pale yellow solution became colourless within 15 minutes, and the reaction mixture was stirred for one day at room temperature. After evaporation of the solvent, the residue was washed with pentane (5 mL). The remaining white solid was dried under vacuum to afford **6** in almost quantitative yield (298 mg, 97%). Crystals suitable for X-ray diffraction analysis were obtained from a mixture of toluene and *n*-hexane at −30 °C. ^{1}H NMR (400 MHz, C_6D_6): δ/ppm 0.82 (s, 9H, CH_3), 1.33 (s, 9H, CH_3), 1.39 (s, 9H, CH_3), 6.24 (s, 1H, C*H*); ^{11}B NMR (128 MHz, C_6D_6): δ/ppm −3.3 (s); ^{13}C NMR (100 MHz, C_6D_6): δ/ppm 28.1 (CH_3, Me (*t*BuNCS)), 29.1 (CH_3, Me), 29.6 (CH_3, Me), 33.4 (C_q, *C*Me$_3$), 34.4 (C_q, *C*Me$_3$), 56.4 (C_q, *C*Me$_3$ (*t*BuNCS)), 111.1 (CH, C═*C*HC), 119.0 (C_q, B*C*$_{ipso}$), 137.7 (C_q, d, $^1J_{CF}$ = 253 Hz *meta*-C_6F_5), 140.9 (C_q, d, $^1J_{CF}$ = 255 Hz *para*-C_6F_5), 146.2 (C_q, N*C*S), 145.8 (C_q, d, $^1J_{CF}$ = 253 Hz, *ortho*-C_6F_5), 156.1 (C_q, N═*C*CCH), 160.5 (C_q, N═*C*CCH); ^{19}F NMR (376 MHz, C_6D_6): δ/ppm −130.9 (m, 4F, *o*-C_6F_5), −156.1 (m, 2F, *p*-C_6F_5), −163.5 (m, 4F, *m*-C_6F_5); elemental analysis (%) calculated for $C_{28}H_{28}BF_{10}N_3S$: C 52.6, H 4.4, N 6.6, found: C 52.3, H 4.6, N 6.2.

Synthesis and characterisation of the MeNCS adduct 7

A toluene solution (5 mL) of **1** (200 mg, 0.38 mmol) was treated with methyl isothiocyanate (28 mg, 0.38 mmol). The mixture was stirred for two days at room temperature. After evaporation of the solvent, the residue was washed with pentane (2 mL). The remaining white solid was dried in vacuum to afford **7** (210 mg, 92%). Crystals suitable for X-ray diffraction analysis were obtained from a mixture of toluene and pentane at −30 °C. ^{1}H NMR (300 MHz, C_6D_6): δ/ppm 0.71 (s, 9H, CH_3), 1.63 (s, 9H, CH_3), 3.09 (s, 3H, CH_3), 6.10 (s, 1H, C*H*); ^{11}B NMR (96 MHz, C_6D_6): δ/ppm −1.8 (s); ^{13}C NMR (75 MHz, C_6D_6): δ/ppm 28.8 (CH_3, Me), 29.9 (CH_3, Me), 32.6 (C_q, *C*Me$_3$), 33.9 (CH_3, Me (MeNCS)), 34.3 (C_q, *C*Me$_3$), 110.0 (CH, C═*C*HC), 137.9 (C_q, d, $^1J_{CF}$ = 251 Hz *meta*-C_6F_5), 141.3 (C_q, d, $^1J_{CF}$ = 254 Hz,

para-C_6F_5), 148.8 (C_q, d, $^1J_{CF}$ = 236 Hz, *ortho*-C_6F_5), 157.8 (C_q, N=*C*CCH), 159.7 (C_q, N=*C*CCH), 171.3 (C_q, N*C*S); ^{19}F NMR (188 MHz, C_6D_6): δ/ppm −134.5 (m, 4F, *o*-C_6F_5), −153.6 (m, $^3J_{FF}$ = 21.0 Hz, 2F, *p*-C_6F_5), −162.2 (m, 4F, *m*-C_6F_5); elemental analysis (%) calculated for $C_{25}H_{22}BF_{10}N_3S$: C 50.3, H 3.7, N 7.0, found: C 50.7, H 3.9, N 6.6.

Synthesis and characterisation of the PhCN adduct 8

A toluene solution (2 mL) of **1** (92 mg, 0.18 mmol) was treated with benzonitrile (18 mg, 0.18 mmol) at room temperature. The pale yellow solution became immediately colourless, and the reaction mixture was stirred for another ten minutes. After evaporation of all volatiles, **8** was isolated as a white solid (93 mg, 85%). Crystals suitable for X-ray diffraction analysis were obtained from a toluene/*n*-hexane mixture at −30 °C. ^{1}H NMR (400 MHz, C_6D_6): δ/ppm 0.79 (br s, 9H, C*H*$_3$), 0.94 (br s, 9H, C*H*$_3$), 6.08 (s, 1H, C*H*), 6.96 (m, 3H, *m*- and *p*-Ph), 7.37 (m, 2H, *o*-Ph); ^{11}B NMR (128 MHz, C_6D_6): δ/ppm 1.9 (s); ^{13}C NMR (100 MHz, C_6D_6): δ/ppm 29.4 (br s, CH_3, Me), 30.4 (br s, CH_3, Me), 31.8 (C_q, *C*Me$_3$), 32.8 (br s, C_q, *C*Me$_3$), 109.2 (CH, C=*C*HC), 116.9 (C_q, B*C*$_{ipso}$), 128.3 (C_q, *m*-Ph), 129.9 (C_q, *o*-Ph), 130.4 (C_q, *p*-Ph), 133.4 (br s, C_q, N*C*Ph), 137.7 (C_q, d, $^1J_{CF}$ = 251 Hz *meta*-C_6F_5), 143.0 (C_q, d, $^1J_{CF}$ = 254 Hz, *para*-C_6F_5), 149.0 (C_q, d, $^1J_{CF}$ = 246 Hz, *ortho*-C_6F_5), 152.3 (br s, C_q, N=*C*CCH), 160.5 (br s, C_q, N=*C*CCH); ^{19}F NMR (376 MHz, C_6D_6): δ/ppm −134.8 (m, 4F, *o*-C_6F_5), −156.7 (m, 2F, *p*-C_6F_5), −163.7 (m, 4F, *m*-C_6F_5); elemental analysis (%) calculated for $C_{30}H_{24}BF_{10}N_3$: C 57.4, H 3.9, N 6.7, found: C 57.6, H 4.2, N 6.5.

Synthesis and characterisation of the *t*BuNC adduct 9

A toluene solution (5 mL) of **1** (250 mg, 0.48 mmol) was treated with *tert*-butyl isocyanide (40 mg, 0.48 mmol) at room temperature. The pale yellow solution became immediately colourless, and the reaction mixture was stirred for 30 minutes. After evaporation of all volatiles, **9** was isolated as a white solid (277 mg, 95%). Crystals suitable for X-ray diffraction analysis were obtained from toluene solution at −30 °C. ^{1}H NMR (300 MHz, C_7D_8): δ/ppm 0.93 (s, 9H, C*H*$_3$), 0.98 (s, 9H, C*H*$_3$), 1.42 (s, 9H, C*H*$_3$), 6.13 (s, 1H, C*H*); ^{11}B NMR (96 MHz, C_7D_8): δ/ppm −9.0 (s); ^{13}C NMR (75 MHz, C_7D_8): δ/ppm 28.3 (CH_3, Me), 30.7 (CH_3, Me), 31.2 (CH_3, Me), 31.8 (C_q, *C*Me$_3$), 32.4 (C_q, *C*Me$_3$), 59.3 (C_q, *C*Me$_3$ (*t*BuNC)), 102.0 (CH, C=*C*HC), 138.3 (C_q, d, $^1J_{CF}$ = 258 Hz *meta*-C_6F_5), C_q *para*-C_6F_5 is not observed, 149.0 (C_q, d, $^1J_{CF}$ = 244 Hz, *ortho*-C_6F_5), 157.5 (C_q, N=*C*CCH), 160.6 (C_q, N=*C*CCH); ^{19}F NMR (188 MHz, C_7D_8): δ/ppm −133.3 (m, 4F, *o*-C_6F_5), −155.4 (m, $^3J_{FF}$ = 20.5 Hz, 2F, *p*-C_6F_5), −163.5 (m, 4F, *m*-C_6F_5); elemental analysis (%) calculated for $C_{28}H_{28}BF_{10}N_3$: C 55.4, H 4.7, N 6.9, found: C 55.3, H 4.5, N 7.1.

Synthesis and characterisation of the PhC≡CH adduct 10

A toluene solution (5 mL) of **1** (118 mg, 0.23 mmol) was treated with phenylacetylene (23 mg, 0.23 mmol) at room temperature. The pale yellow solution became immediately colourless, and the reaction was stirred for two hours. After evaporation of the solvent, the residue was washed with pentane (5 mL), and the remaining white solid was dried in vacuum (120 mg, 83%). Crystals suitable for X-ray diffraction analysis were obtained from toluene solution at −30 °C. ^{1}H NMR (400 MHz, C_7D_8): δ/ppm 0.89 (s, 9H, C*H*$_3$), 0.92 (s, 9H, C*H*$_3$), 5.96 (d, $^4J_{HH}$ = 2.7 Hz 1H, C*H*), 6.93 (m, 3H, *m*- and *p*-Ph), 7.42 (m, 2H, *o*-Ph), 12.20 (br s, 1H, N*H*); ^{11}B NMR (128 MHz, C_7D_8): δ/ppm −8.9 (s); ^{13}C NMR (100 MHz, C_7D_8): δ/ppm 29.0 (CH_3, Me), 29.7 (CH_3, Me), 31.22 (C_q, *C*Me$_3$), 33.0 (C_q, *C*Me$_3$), 102.4 (C_q, Ph-*C*C)), 104.7 (CH, C=*C*HC), 124.8 (C_q, *i*-Ph), 128.5 (C_q, *p*-Ph), 128.5 (C_q, *m*-Ph), 131.7 (C_q, *o*-Ph), 137.8 (C_q, d, $^1J_{CF}$ = 252 Hz *meta*-C_6F_5), C_q *para*-C_6F_5 is not observed, 148.9 (C_q, d, $^1J_{CF}$ = 239 Hz, *ortho*-C_6F_5), 153.9 (C_q, N=*C*CCH), 162.5 (C_q, N=*C*CCH); ^{19}F NMR (376 MHz, C_7D_8): δ/ppm −133.7 (m, 4F, *o*-C_6F_5), −157.5 (m, $^3J_{FF}$ = 20.0 Hz, 2F, *p*-C_6F_5), −164.1 (m, 4F, *m*-C_6F_5); elemental analysis (%) calculated for $C_{31}H_{25}BF_{10}N_2$: C 59.5, H 4.0, N 4.5, found: C 59.3, H 4.2, N 4.4.

X-Ray diffraction studies

X-Ray diffraction analysis data were recorded at 100 K on Oxford Diffraction diffractometers using monochromated Mo-Kα or mirror-focussed Cu-Kα radiation. The structures were refined anisotropically on F^2 using the SHELX-97 program.[36] Absorption corrections were based on multi-scans. Hydrogen atoms were included using rigid idealized methyl groups or a riding model. Crystallographic data are summarized in Table 1. *Exceptions and special features*: compounds **4** and **9** crystallized with a molecule of toluene disordered across an inversion centre. For **4** this could not be satisfactorily refined, and the effects of the solvent were therefore removed with the program SQUEEZE;[37] for **9** a disorder model involving an idealized aromatic ring was successfully employed. One C_6F_5 ring of compound **8** is disordered over two positions with occupancies 0.788/0.212(4). An appropriate system of restraints was used to improve refinement stability, but the dimensions of disordered groups should always be interpreted with caution. For compound **10**, the NH hydrogen was refined freely; the toluene molecule is well-ordered.

Theoretical calculations

The calculations were performed using the *GAUSSIAN09* package.[38] All structures were fully optimized on the density functional theory (DFT) level employing the M06-2X functional.[39] For all elements (C, H, B, N and F) the all-electron triple-ζ basis set (6-311++G**) was used.[40] Additional details of the electronic structure calculations and presentations of all calculated structures together with Cartesian coordinates of their atomic positions are provided as ESI.†

Acknowledgements

This work is supported by the Deutsche Forschungsgemeinschaft (DFG) through grant Ta 189/9-1 and by the Deutsche

Table 1 Crystallographic data

	3	**4**·1/2(toluene)	**5**	**6**	**7**	**8**	**9**·1/2(toluene)	**10**·toluene
Empirical formula	$C_{24}H_{19}BF_{10}N_2O_2$	$C_{27.5}H_{25}BF_{10}N_2O$	$C_{28}H_{28}BF_{10}N_3O$	$C_{28}H_{28}BF_{10}N_3S$	$C_{25}H_{22}BF_{10}N_3S$	$C_{30}H_{24}BF_{10}N_3$	$C_{31.5}H_{32}BF_{10}N_3$	$C_{38}H_{33}BF_{10}N_2$
Formula weight	568.22	600.30	623.34	639.40	597.33	627.33	653.41	718.47
T/K	100(2)	100(2)	100(2)	100(2)	100(2)	100(2)	100(2)	100(2)
Wavelength λ/Å	0.71073	1.54184	0.71073	1.54184	1.54184	0.71073	0.71073	1.54184
Crystal system	Monoclinic	Triclinic	Monoclinic	Monoclinic	Monoclinic	Monoclinic	Triclinic	Triclinic
Space group	$C2/c$	$P\bar{1}$	$P2_1/n$	$P2_1/n$	$P2_1/c$	$P2_1/n$	$P\bar{1}$	$P\bar{1}$
a/Å	15.3482(4)	9.2377(6)	10.9606(4)	11.1232(2)	10.1128(2)	11.8154(3)	9.5902(12)	11.0480(6)
b/Å	14.1117(4)	11.5573(10)	19.1668(6)	13.5996(2)	12.5196(2)	15.1224(5)	11.3185(16)	13.2011(7)
c/Å	23.0099(6)	13.2013(12)	14.3458(4)	19.3628(2)	20.7678(4)	15.9346(5)	15.1442(18)	13.2014(7)
α (°)	90	73.287(8)	90	90	90	90	85.961(10)	73.524(5)
β (°)	108.656(4)	86.450(6)	102.930(4)	96.913(2)	97.885(2)	97.556(3)	88.454(10)	69.985(5)
γ (°)	90	83.350(6)	90	90	90	90	74.367(12)	78.473(5)
Volume [Å^3]	4721.8(2)	1340.18(19)	2937.34(16)	2907.4(7)	2604.51(8)	2822.43(15)	1586.5(4)	1723.48(16)
Z	8	2	4	4	4	4	2	2
Reflections collected	95 441	14 213	106 116	54 092	41 673	67 513	36 032	63 138
Independent reflections	4817 [R_{int} = 0.0475]	5492 [R_{int} = 0.0181]	7000 [R_{int} = 0.0554]	5941 [R_{int} = 0.0272]	5324 [R_{int} = 0.0289]	4972 [R_{int} = 0.0515]	6468 [R_{int} = 0.0827]	7144 [R_{int} = 0.0222]
ρ_C/g cm^{-3}	1.599	1.488	1.410	1.461	1.523	1.476	1.368	1.384
μ/mm^{-1}	0.155	1.218	0.130	1.795	1.962	0.133	0.121	1.022
$R(F_O)$, [$I > 2\sigma(I)$]	0.0322	0.0332	0.0426	0.0283	0.0289	0.0371	0.0506	0.0326
Rw (F_O^2)	0.0740	0.0929	0.0983	0.0735	0.0784	0.0854	0.1187	0.0849
Goodness of fit on (F^2)	1.011	1.051	1.028	1.048	1.037	1.034	1.029	1.038
$\Delta\rho$/eÅ^{-3}	0.297/−0.223	0.241/−0.197	0.321/−0.300	0.285/−0.222	0.291/−0.210	0.298/−0.244	0.251/−0.241	0.378/−0.258

Bundesstiftung Umwelt (DBU) through a scholarship for E. Theuergarten.

Notes and references

1 (*a*) A. L. Kenward and W. E. Piers, *Angew. Chem., Int. Ed.*, 2008, **47**, 38; (*b*) D. W. Stephan, *Org. Biomol. Chem.*, 2008, **6**, 1535; (*c*) D. W. Stephan, *Dalton Trans.*, 2009, 3129; (*d*) D. W. Stephan and G. Erker, *Angew. Chem., Int. Ed.*, 2010, **49**, 46.

2 G. C. Welch, R. R. San Juan, J. D. Masuda and D. W. Stephan, *Science*, 2006, **314**, 1124.

3 Selected articles: (*a*) G. C. Welch and D. W. Stephan, *J. Am. Chem. Soc.*, 2007, **129**, 1880; (*b*) A. L. Kenward and W. E. Piers, *Angew. Chem., Int. Ed.*, 2008, **47**, 38; (*c*) D. P. Huber, G. Kehr, K. Bergander, R. Fröhlich, G. Erker, S. Tanino, Y. Ohki and K. Tatsumi, *Organometallics*, 2008, **27**, 5279; (*d*) V. Sumerin, F. Schulz, M. Nieger, M. Leskelä, T. Repo and B. Rieger, *Angew. Chem., Int. Ed.*, 2008, **47**, 6001; (*e*) T. Rokob, A. Hamza and I. Papai, *J. Am. Chem. Soc.*, 2009, **131**, 10701; (*f*) D. W. Stephan, *Chem. Commun.*, 2010, **46**, 8526.

4 (*a*) H. Wang, R. Fröhlich, G. Kehr and G. Erker, *Chem. Commun.*, 2008, 5966; (*b*) S. J. Geier, T. M. Gilbert and D. W. Stephan, *J. Am. Chem. Soc.*, 2008, **130**, 12632; (*c*) M. Ullrich, A. J. Lough and D. W. Stephan, *J. Am. Chem. Soc.*, 2009, **131**, 52; (*d*) R. C. Neu, E. Y. Ouyang, S. J. Geier, X. Zhao, A. Ramos and D. W. Stephan, *Dalton Trans.*, 2010, **39**, 4285; (*e*) M. Harhausen, R. Fröhlich, G. Kehr and G. Erker, *Organometallics*, 2012, **31**, 2801.

5 (*a*) C. Jiang, O. Blacque and H. Berke, *Organometallics*, 2009, **28**, 5233; (*b*) S. J. Geier and D. W. Stephan, *J. Am. Chem. Soc.*, 2009, **131**, 3476; (*c*) F. Schulz, V. Sumerin, M. Leskel, T. Repo and B. Rieger, *Dalton Trans.*, 2010, **39**, 1920; (*d*) G. Erős, H. Mehdi, I. Pápai, T. A. Rokob, P. Király, G. Tárkányi and T. Soós, *Angew. Chem., Int. Ed.*, 2010, **49**, 6559; (*e*) C. Jiang, O. Blacque, T. Fox and H. Berke, *Dalton Trans.*, 2011, **40**, 1091; (*f*) C. B. Caputo, S. J. Geier, D. Winkelhaus, N. W. Mitzel, V. N. Vukotic, S. J. Loeb and D. W. Stephan, *Dalton Trans.*, 2012, **41**, 2131.

6 (*a*) D. Holschumacher, T. Bannenberg, C. G. Hrib, P. G. Jones and M. Tamm, *Angew. Chem., Int. Ed.*, 2008, **47**, 7428; (*b*) D. Holschumacher, C. Taouss, T. Bannenberg, C. G. Hrib, C. G. Daniliuc, P. G. Jones and M. Tamm, *Dalton Trans.*, 2009, 6927; (*c*) S. Kronig, E. Theuergarten, D. Holschumacher, T. Bannenberg, C. G. Daniliuc, P. G. Jones and M. Tamm, *Inorg. Chem.*, 2011, **50**, 7344; (*d*) S. Kronig, E. Theuergarten, C. G. Daniliuc, P. G. Jones and M. Tamm, *Angew. Chem., Int. Ed.*, 2012, **51**, 3240.

7 (*a*) P. A. Chase and D. W. Stephan, *Angew. Chem., Int. Ed.*, 2008, **47**, 7433; (*b*) P. A. Chase, A. L. Gille, T. M. Gille and D. W. Stephan, *Dalton Trans.*, 2009, 7179.

8 M. Alcarazo, C. Gomez, S. Holle and R. Goddard, *Angew. Chem., Int. Ed.*, 2010, **49**, 5788.

9 (*a*) G. Ménard and D. W. Stephan, *J. Am. Chem. Soc.*, 2010, **132**, 1796; (*b*) Y. Zhang, G. M. Miyake and E. Y.-X. Chen, *Angew. Chem., Int. Ed.*, 2010, **49**, 10158.

10 A. Schäfer, M. Reißmann, A. Schäfer, W. Saak, D. Haase and T. Müller, *Angew. Chem., Int. Ed.*, 2011, **50**, 12636.

11 A. M. Chapman, M. F. Haddow and D. F. Wass, *J. Am. Chem. Soc.*, 2011, **133**, 18463.

12 (*a*) K. V. Axenov, C. M. Mömming, G. Kehr, R. Fröhlich and G. Erker, *Chem.–Eur. J.*, 2010, **16**, 14069; (*b*) Z. M. Heiden, M. Schedler and D. W. Stephan, *Inorg. Chem.*, 2011, **50**, 1470; (*c*) S. Schwendemann, R. Fröhlich, G. Kehr and G. Erker, *Chem. Sci.*, 2011, **2**, 1842.

13 (*a*) P. Spies, G. Erker, G. Kehr, K. Bergander, R. Fröhlich, S. Grimme and D. W. Stephan, *Chem. Commun.*, 2007, 5072; (*b*) P. Spies, G. Kehr, K. Bergander, B. Wibbeling, R. Fröhlich and G. Erker, *Dalton Trans.*, 2009, 1534.

14 (*a*) V. Sumerin, F. Schulz, M. Nieger, C. Wang, M. Leskelä, P. Pyykkö, T. Repo and B. Rieger, *J. Organomet. Chem.*, 2009, **694**, 2654; (*b*) V. Sumerin, F. Schulz, M. Atsumi, C. Wang, M. Nieger, M. Leskelä, T. Repo, P. Pyykkö and B. Rieger, *J. Am. Chem. Soc.*, 2008, **130**, 14117.

15 D. W. Stephan, S. Greenberg, T. W. Graham, P. Chase, J. J. Hastie, S. J. Geier, J. M. Farrell, C. C. Brown, Z. M. Heiden, G. C. Welch and M. Ullrich, *Inorg. Chem.*, 2011, **50**, 12338.

16 G. Lu, H. Li, L. Zhao, F. Huang and Z.-X. Wang, *Inorg. Chem.*, 2010, **49**, 295.

17 E. Theuergarten, D. Schlüns, J. Grunenberg, C. G. Daniliuc, P. G. Jones and M. Tamm, *Chem. Commun.*, 2010, **46**, 8561.

18 C. M. Mömming, S. Frömel, G. Kehr, R. Fröhlich, S. Grimme and G. Erker, *J. Am. Chem. Soc.*, 2009, **131**, 12280.

19 C. M. Mömming, G. Kehr, B. Wibbeling, R. Fröhlich, B. Schirmer, S. Grimme and G. Erker, *Angew. Chem., Int. Ed.*, 2010, **49**, 2414.

20 F. Bertini, V. Lyaskovskyy, B. J. J. Timmer, F. J. J. de Kanter, M. Lutz, A. W. Ehlers, J. C. Slootweg and K. Lammertsma, *J. Am. Chem. Soc.*, 2012, **134**, 201.

21 C. M. Mömming, E. Otten, G. Kehr, R. Fröhlich, S. Grimme, D. W. Stephan and G. Erker, *Angew. Chem., Int. Ed.*, 2009, **48**, 6643.

22 C. M. Mömming, G. Kehr, B. Wibbeling, R. Fröhlich and G. Erker, *Dalton Trans.*, 2010, **39**, 7556.

23 S. Porcel, G. Bouhadir, N. Saffon, L. Maron and D. Bourissou, *Angew. Chem., Int. Ed.*, 2010, **49**, 6186.

24 (*a*) C. Rosorius, G. Kehr, R. Fröhlich, S. Grimme and G. Erker, *Organometallics*, 2011, **30**, 4211; (*b*) A. Stute, G. Kehr, R. Fröhlich and G. Erker, *Chem. Commun.*, 2011, **47**, 4288.

25 (*a*) J. Boudreau, M.-A. Courtemanche and F.-G. Fontaine, *Chem. Commun.*, 2011, **47**, 11131; (*b*) C. Appelt, H. Westenberg, F. Bertini, A. W. Ehlers, J. C. Slootweg, K. Lammertsma and W. Uhl, *Angew. Chem., Int. Ed.*, 2011, **50**, 3925.

26 M. A. Dureen and D. W. Stephan, *J. Am. Chem. Soc.*, 2010, **132**, 13559.

27 A. E. Ashley, A. L. Thompson and D. O`Hare, *Angew. Chem., Int. Ed.*, 2009, **48**, 9839.

28 A. Berkefeld, W. E. Piers and M. Parvez, *J. Am. Chem. Soc.*, 2010, **132**, 10660.

29 S. D. Tran, T. A. Tronic, W. Kaminsky, D. M. Heinekey and J. M. Mayer, *Inorg. Chim. Acta*, 2011, **369**, 126.

30 R. G. Pearson, *J. Am. Chem. Soc.*, 1963, **85**, 3533.

31 F. H. Allen, O. Kennard and D. G. Watson, *J. Chem. Soc., Perkin Trans. 2*, 1987, 1.

32 (*a*) M. Tamm and F. E. Hahn, *Coord. Chem. Rev.*, 1999, **182**, 175; (*b*) E. Singleton and H. E. Oosthuizen, *Adv. Organomet. Chem.*, 1983, **22**, 209; (*c*) P. M. Treichel, *Adv. Organomet. Chem.*, 1973, **11**, 21.

33 M. Tamm, T. Lügger and F. E. Hahn, *Organometallics*, 1996, **15**, 1251.

34 H. Jacobsen, H. Berke, S. Döring, G. Kehr, G. Erker, R. Fröhlich and O. Meyer, *Organometallics*, 1999, **18**, 1724.

35 M. A. Dureen and D. W. Stephan, *J. Am. Chem. Soc.*, 2009, **131**, 8396.

36 G. M. Sheldrick, *Acta Crystallogr., Sect. A: Found. Crystallogr.*, 2008, **A64**, 112.

37 A. L. Spek, *SQUEEZE forms part of the PLATON program suite*, University of Utrecht, Netherlands, 2009.

38 M. J. Frisch, *GAUSSIAN 09 (Revision A.1)*, Gaussian, Inc., Wallingford, CT, 2009.

39 (*a*) Y. Zhao and D. G. Truhlar, *Theor. Chem. Acc.*, 2008, **120**, 215; (*b*) Y. Zhao and D. G. Truhlar, *Acc. Chem. Res.*, 2008, **41**, 157.

40 R. Krishnan, J. S. Binkley, R. Seeger and J. A. Pople, *J. Chem. Phys.*, 1980, **72**, 650.

